Title

Reversible Homolysis of a Carbon-Carbon σ-Bond Enabled by Complexation-Induced Bond-Weakening.

Journal

Journal of the American Chemical Society, 144(34)

Authors

Kim, Suhong
Chen, Pan-Pan
Knowles, Robert
et al.

Publication Date

2022-08-31

DOI

10.1021/jacs.2c01229

Peer reviewed

Published in final edited form as:

J Am Chem Soc. 2022 August 31; 144(34): 15488–15496. doi:10.1021/jacs.2c01229.

Reversible Homolysis of a Carbon–Carbon σ-Bond Enabled by Complexation-Induced Bond-Weakening

Suhong Kim[a], **Pan-Pan Chen**[b], **K. N. Houk**[b], **Robert R. Knowles**[a]

[a]Department of Chemistry, Princeton University, Princeton, New Jersey 08544, United States

[b]Department of Chemistry and Biochemistry, University of California, Los Angeles, California 90095, United States

Abstract

A case study of catalytic carbon–carbon σ-bond homolysis is presented. The coordination of a redox-active Lewis acid catalyst reduces the bond-dissociation free energies of adjacent carbon–carbon σ-bonds, and this complexation-induced bond-weakening is used to effect reversible carbon–carbon bond homolysis. Stereochemical isomerization of 1,2-disubstituted cyclopropanes was investigated as a model reaction with a ruthenium (III/II) redox couple adopted for bond weakening. Results from our mechanistic investigation into the stereospecificity of the isomerization reaction are consistent with selective complexation-induced carbon–carbon bond homolysis. The $\Delta G^{\ddagger}$ of catalyzed and uncatalyzed reactions were estimated to be 14.4 kcal/mol and 40.0 kcal/mol, respectively with the computational method, (U)PBE0-D3/def2-TZVPP-SMD(toluene)//(U)B3LYP-D3/def2-SVP. We report this work as the first catalytic example where the complexation-induced bond-weakening effect is quantified through transition state analysis.

Graphical Abstract

Corresponding Author: Robert R. Knowles − Department of Chemistry, Princeton, University, Princeton, New Jersey 08544, United States; rknowles@princeton.edu, K. N. Houk − Department of Chemistry and Biochemistry, University of California, Los Angeles, California 90095, United States, houk@chem.ucla.edu.

ASSOCIATED CONTENT

Supporting Information

The Supporting Information is available free of charge on the ACS Publications website.

Experimental procedures and characterization data; coordinates and energies of DFT-computed stationary points (PDF).

Accession Codes

CCDC 2084242 contains the supplementary crystallographic data for this paper. These data can be obtained free of charge via www.ccdc.cam.ac.uk/data_request/cif, or by emailing data_request@ccdc.cam.ac.uk, or by contacting The Cambridge Crystallographic Data Centre, 12 Union Road, Cambridge CB2 1EZ, UK; fax: +44 1223 336033.

The authors declare no competing financial interest.

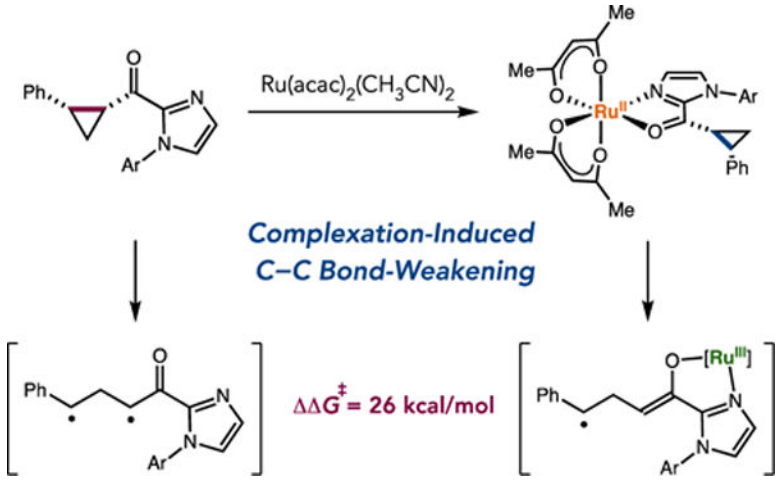

INTRODUCTION

Over the past decade, transition metal-catalyzed carbon–carbon bond activation has emerged as an enabling technology in organic synthesis.[1–5] In general, the cleavage of C–C bonds with transition metal catalysts is achieved through either oxidative addition[6–10] (Scheme 1A) or β-carbon elimination[11–14] (Scheme 1B). After insertion into a C–C σ-bond, the resulting organometallic intermediate can be subsequently functionalized through C–H, C–C, or C–X bond-forming reactions. While powerful, the scope of these processes remains limited, and the downstream chemistry of the metal intermediates is generally limited to two-electron processes. In considering alternative approaches to catalytic C–C bond cleavage chemistry, we became intrigued by the possibility of transition metal-catalyzed C–C bond homolysis through complexation-induced bond-weakening (Scheme 1C).

Bond-weakening is a well-known phenomenon in organometallic chemistry wherein the bond-dissociation free energies (BDFEs) of bonds in associated ligands are decreased upon coordination to a reducing metal center.[15–18] The origin of bond-weakening is the coupling of the homolytic bond cleavage event with a favorable oxidation state change at the metal center. These effects have been observed for numerous combinations of metal and ligand, with significant weakening of O–H, N–H, and even C–H bonds (Figure 1).[19–23] While this favorable ET process can conceivably be coupled with other homolysis events, the applications of bond-weakening remain generally limited to the activation of X–H type σ-bonds.[24,25] Accordingly, in this study, we attempt to extend and adapt these bond weakening concepts as a platform for C–C bond cleavage as well.

Here, we present a ruthenium-catalyzed stereochemical isomerization of 1,2-disubstituted cyclopropanes as a case study for complexation-induced bond-weakening catalysis. A variety of mechanistic studies suggest C–C σ-bond homolysis as the key elementary step in the interconversion of cyclopropane stereoisomers. In addition, while bond-weakening is typically discussed and analyzed in thermodynamic terms, in this report we provide a quantitative analysis of its impact on the kinetic barriers for C–C bond cleavage.

Background of Cyclopropane C–C Bond Homolysis.

The pyrolysis of small ring hydrocarbons has historically served as an ideal model system to investigate the homolytic activation of C–C σ-bonds.[26] Since the initial work of Trautz and Winkler in 1922, cyclopropanes have remained an attractive system to study because the comparatively low temperatures required for their C–C bond cleavage chemistry (350 °C ~ 450 °C) relative to other acyclic hydrocarbons (550 °C ~ 650 °C) allowed for more precise kinetic analysis.[27]

Following the work of Chambers and Kistiakowsky in 1934 detailing a mechanistic study of 'structural isomerization' of cyclopropane to propylene,[28] Rabinovitch, Schlag, and Wiberg reported the 'geometric isomerization' (*cis–trans* interconversion) of 1,2-dideuteriocyclopropanes in 1958.[29] In this study, the authors were able to demonstrate that C–C bond cleavage was the operative mechanism for isomerization in preference to hydrogen atom migration. A decade later, Berson and Bergman independently published reports on 'optical isomerization' of (+)-*trans*-tetramethylcyclopropane-d_6 and (–)-*cis*-1-methyl-2-ethylcyclopropane, respectively.[30,31] Kinetic analysis of the relative rates of both geometric and optical isomerization identified nonpolar 1,3-diradical species as the common intermediates of the overall isomerization process. Importantly, these studies also validated the reversibility of C–C bond homolytic cleavage based on the competition between intramolecular radical recombination and bond rotation. In addition, the precise measurement of the activation barriers for bond scission delineated the upper limit for the BDFE of various cyclopropane derivative C–C σ-bonds (Figure 2A).[32]

Drawing inspiration from these early works, we elected to focus on cyclopropane derivatives as model systems for complexation-induced C–C bond cleavage. In this context, we were particularly drawn to a report from Tanko and Drumlight that provided evidence for the reversible ring opening of aryl cyclopropyl ketyl radical anions (Figure 2B). These authors concluded that the observed reversibility originates from the stability of ketyl anion intermediates.[33] Subsequent studies showed that the driving force of cyclopropylcarbinyl rearrangement depends on the substrate substitution patterns.[34] In particular, the ring-opening of phenyl cyclopropyl ketyl anion is endergonic while that of phenyl 2-phenylcyclopropyl ketyl anion is exergonic.

These studies demonstrate that modulating the electronic nature of adjacent functional groups impacts the thermodynamics of ring-opening/ring-closing processes and, therefore, influences the BDFEs of cyclopropane C–C σ-bonds. Accordingly, we hypothesized that coordination of redox-active Lewis acid catalysts would also modulate the BDFEs of the cyclopropane C–C σ-bonds and thus influence the homolysis event in an analogous manner. This hypothesis led us to examine complexation-induced bond-weakening of C–C σ-bonds by using a cyclopropyl 2-imidazolyl ketone as a model substrate.

Design of Catalytic System.

In an effort to identify a catalytic system involving complexation-induced C–C bond homolysis, we considered the unique features of N–H bond weakening observed with ruthenium bis(β-diketonato) complexes reported by Mayer and co-workers (Figure

3A).[35] In comparison with their previous study on homoleptic iron tris(α-diimine) complexes,[36,37] the heteroleptic ruthenium complexes were prepared by ligand substitution with 2-(2'-pyridyl)imidazole from the corresponding acetonitrile-bound ruthenium complex $Ru(acac)_2(CH_3CN)_2$. This precedent demonstrates the possibility of using $Ru(acac)_2(CH_3CN)_2$ as the precatalyst for our desired reaction and the feasibility of catalyst turnover if the binding of substrate is reversible. This system was especially attractive due to its diamagnetic character allowing for reaction monitoring by NMR spectroscopy.

We focused on geometric (*cis, trans*) isomerization and initiated our screening of catalytic reaction conditions (Figure 3B). Results from structural isomerization could be confounded by the involvement of other elementary steps such as C–O bond formation. Optical isomerization was studied later with conditions optimized from our geometric isomerization studies (*vide infra*).

The prospective catalytic cycle for the isomerization reaction is delineated in Scheme 2. We propose that the phenylcyclopropyl ketone substrate tethered to the imidazole directing group could coordinate to the $Ru(acac)_2$ catalyst, resulting in a decrease in the BDFE of the cyclopropane C–C σ-bond. When sufficient thermal energy is provided upon heating, this bond-weakening effect would promote C–C σ-bond homolysis under relatively mild conditions to generate an open-shell intermediate. If the intermediate persists long enough to allow for bond rotation prior to recombination, then the interconversion of diastereomers would be observed. As observed in the reversible binding of 1-phenyl-imidazol-2-yl methyl ketone, we assumed the binding of substrate and product is reversible, enabling the catalyst to be turned over via ligand exchange.

RESULTS AND DISCUSSION

Effect of Reaction Parameters.

In our preliminary optimization, we were able to increase the conversion and yield to a satisfactory level for further mechanistic investigation. By using 5.2 mol% of $Ru(acac)_2(CH_3CN)_2$ as the catalyst, 91% of **1** was converted to 81% of **2** upon heating to 80 °C in trifluorotoluene (Table 1, entry 1). The remaining mass balance is predominantly an isomerized product, yet trace amounts of other uncharacterized side products are also formed. Notably, the dihydrofuran byproduct would arise from the same C–C bond cleavage mechanism as the proposed *cis* to *trans* isomerization. We performed further variable screening to determine how the change of reaction conditions influenced the reaction outcome. The results of these control experiments are listed in Table 1.

While gentle heating was sufficient for catalysis, no conversion was observed at ambient temperature (Table 1, entry 2). This was an encouraging result in light of a report from Doering and Sachdev disclosing incomplete thermal rearrangement of methyl 2-isopropenylcyclopropane-l-carboxylate at 280 °C (Scheme 3).[38] Such a large temperature difference between the uncatalyzed pyrolysis conditions and our reaction conditions demonstrates the promising utility of bond-weakening catalysis as a mild method to generate radical intermediates.

We found that when the catalyst loading, concentration, and reaction time are unchanged, higher temperature led to higher conversion, but not to a higher yield of **2** (entries 3, 4). This result suggests the existence of undesired reaction pathways either from **2** or directly from **1** at elevated temperature. Higher concentrations of **1** also resulted in greater conversion but not necessarily higher yields of **2** (entries 5, 6). Screening of catalyst loading and reaction time also suggested that the maximum yield was obtained when the conversion approaches approximately 90%. After this point, further conversion of substrate is accompanied by competitive decomposition (entries 7–11). The reaction tolerates aprotic non-polar solvents, such as aromatic and ethereal solvents but not dichloromethane (entries 12–16). In addition, the rate and yield are insensitive to the dielectric constant of the solvent, consistent with the involvement of neutral, non-polar intermediates. Lastly, the oxidized and more Lewis acidic complex $[Ru^{III}(acac)_2(CH_3CN)_2]PF_6$ does not catalyze the isomerization to a measurable extent (entry 17).

Stereochemical Probes.

We undertook further mechanistic studies to evaluate whether the observed isomerization is indeed operating by complexation-induced C–C bond-weakening. In this regard, a sequence of stereochemical probe experiments proved particularly informative. A notable observation from the control experiments above is that **2** decomposes significantly after the conversion approaches 90%. Because both **1** and **2** are stable at 80 °C in the absence of catalyst (Table 1, entry 7), we questioned whether **2** might also be subject to further reaction with the Ru catalyst. We validated this assumption by submitting enantioenriched **2** to the standard reaction conditions and observed complete racemization with 77% recovery (Scheme 4).

As this experiment indicates that the C–C σ-bond of **2** is also activated by the Ru catalyst, we proposed that this isomerization process may be fully reversible, with the ratio of **1**:**2** determined by a thermodynamic equilibrium that is independent of the initial isomer ratio. Indeed, we found that reactions of both pure (±)-**1** and pure (±)-**2** both gave a 3:74 ratio of **1**:**2** after 6 hours at 80 °C in the presence of the Ru catalyst. (Scheme 5).

If the racemization of **2** (Scheme 4) and the *cis*- to *trans*-interconversion proceed through an identical activation mode with a common intermediate, then any **2** obtained from enantioenriched **1** should be generated as a racemate (*cf.* Scheme 5). Subsequently, we decided to test the stereospecificity of *cis* to *trans* isomerization (Scheme 6). When enantiopure **1** was reacted under the standard conditions, 51% of racemic **2** was obtained at 62% conversion after 1 hour, and the enantiomeric excess of the recovered substrate was 95%. This result implies that the regeneration of **1** from the intermediate (*i.e.*, the reverse of step #1) is minimal relative to the forward reaction to give **2**. Even though the activation of **1** is reversible, at 62% conversion, only 1.9% (0.38 × 0.05) of *cis* substrate is racemized. Based on this observation, we concluded the regeneration of **1** is negligible at low conversion, and this understanding encouraged us to undertake initial rate kinetic studies (*vide infra*).

Continuing our stereochemical studies, we sought to investigate the selectivity of complexation-induced C–C σ-bond homolysis. Although the reversible bond-breaking and

bond-forming of the σ-bond between the benzylic carbon and α-carbonyl carbon was the simplest mechanism for the observed isomerization, we were also mindful that other combinations of bond-breaking and bond-forming events could potentially be operative. We prepared enantiopure 1,2,3-trisubstituted cyclopropane substrate **3**, which introduces a methyl group to the remaining carbon of cyclopropane ring (Scheme 7), and used it to test the chemoselectivity of the bond scission. The isomerized products **4** and **5** were both formed as single enantiomers, indicating that only one of the three σ-bonds was reversibly activated. Notably, such selectivity of bond-activation is not trivial under the pyrolysis conditions of simple cyclopropanes (*vide supra*).

Kinetic Analysis.

We next turned our attention to understanding the kinetics of this process. Fortunately, the regeneration of substrate from the proposed catalytic intermediate was insignificant until 62% conversion (Scheme 6). At that conversion point, the k_2/k_{-1} value was estimated as 27 (51 ÷ 1.9) by calculating the relative ratio of the product and the racemized substrate. Based on the estimated k_2/k_{-1}, we assumed that less than 0.25% of substrate is made by the rebound from the open-shell intermediate when the conversion is 10%. As this amount of the reformed substrate **1** was negligible compared to the 90% of unreacted substrate **1**, we assumed that the catalytic reaction is effectively irreversible at less than 10% conversion of substrate.

Using the method of initial rates, we found that the reactions showed first-order kinetic dependence on the Ru catalyst in accordance with the proposed bond-weakening catalysis (Figure 4). We then investigated the rate dependence on the substrate concentration (Figure 5) and observed significant deviation from linearity, suggestive of saturation kinetics. Indeed, a linear correlation was observed in a Lineweaver-Burk analysis between the inverse of the initial rates and the inverse of the substrate concentration (Figure 6).

As the reaction follows Michaelis-Menten kinetics, we concluded the binding of the ruthenium catalyst to the substrate is reversible as predicted, and the complexation-induced C–C σ-bond homolysis is the turnover limiting step of the catalytic cycle at low conversion. The Michaelis constant, K_M, and the catalytic rate constant, k_{cat}, are calculated to be 5.82×10^{-2} M and 2.17×10^{-2} s^{-1}, respectively. Accordingly, the catalytic efficiency constant, k_{cat}/K_M, is calculated to be 3.73×10^{-1} $M^{-1}s^{-1}$. In addition, no induction period was observed, indicating that acetonitrile is readily displaced by the bidentate substrate.

Having identified the turnover-limiting step of catalysis, we next set out to measure the activation parameters of the isomerization by probing the temperature dependence of the initial rates. We measured the activation barrier of Ru-catalyzed *cis* to *trans* isomerization via Arrhenius analysis to be 23.2 kcal/mol (Figure 7). This value represents the upper bound for the C–C BDFE in the Ru complexed substrate. Because the activation barrier for thermal isomerization reactions of an electronically analogous substrate is 47.5 ± 2.5 kcal/mol (Scheme 3), we concluded that the complexation of the redox-active $Ru(acac)_2$ Lewis acid is responsible for lowering the activation barrier of the C–C σ-bond homolysis by approximately 24 kcal/mol.

As a potential alternative to bond-weakening, we also questioned whether the *cis* to *trans* isomerization could be mediated by outer-sphere electron transfer from the Ru(II) catalyst to substrate **1**. Because ring-opening of cyclopropyl ketyl anions is reversible (Figure 2B), we hypothesized that the ketyl anion intermediate generated by single-electron reduction of the substrate could also undergo reversible ring-opening reactions. In this case, the catalyst turnover step would be back electron transfer from the ketyl anion intermediate of the product to the Ru(III) state of the catalyst. However, thermodynamic considerations argue against a direct ET-based mechanism. For simple phenyl ketone derivatives of complexes **1** and **2**, the reduction potential ($E_{1/2}$) was measured to be −2.6 V versus $Cp_2Fe^{+/0}$.[33] However, the $Ru^{III/II}$ reduction potential of the compound described in Figure 3A is only −0.64 V suggesting that the electron transfer from the Ru(II) catalyst to the substrate is highly disfavored.[35] As such, a free ketyl radical anion is not a plausible intermediate in the *cis* to *trans* isomerization, and the observed reversibility in the C–C σ-bond homolysis is presumably mediated by coordination of the Ru(II) catalyst.

Homolysis versus Heterolysis.

After measuring the activation barrier, we sought to examine the electronic character of the key C–C bond breaking process through a Hammett analysis. As cyclopropane C–C σ-bond activation is involved in the turnover limiting step, we investigated the influence of the *para*-substituents of the aryl group on the initial reaction rate. We found both electron-withdrawing and electron-donating groups increased the rate of the *cis* to *trans* isomerization. Both a benzylic cation and a benzylic anion were ruled out as intermediates of ruthenium-catalyzed *cis* to *trans* isomerization as neither σ+ nor σ– exhibited linear correlations with the observed reaction rates (see supporting information).[39]

We next turned our attention to correlation with the σ• parameter. Historically, several transformations have been inspected as probes for free radical substituent effects, but there are numerous scales, and the substituent constants vary depending on the nature of the radical intermediate as well as the method of radical generation. We opted to utilize Jackson's improved σ• scale for the extended Hammett equation ($\log (k_X/k_H) = \rho\sigma + \rho^{\bullet}\sigma^{\bullet}$) which was defined through competitive thermal decomposition of substituted dibenzylmercury compounds (see supporting information).[40,41] The parameters ρ and ρ• were calculated to be 0.028 and 0.21, respectively. This outcome indicates that any polar influence is minimal, and that appreciable radical character is developed in the transition state of the bond-activation step. Taken together, all the evidence presented above suggests the generation of a benzylic radical intermediate in the Ru-catalyzed *cis* to *trans* isomerization.

DFT Calculations.

With experimental support for the open-shell intermediate formed from complexation-induced C–C bond homolysis, we assessed the free energy changes of activation of uncatalyzed C–C bond homolysis of **1** through density functional theory calculations with the (U)PBE0-D3/def2-TZVPP-SMD(toluene)//(U)B3LYP-D3/def2-SVP level of theory.[42] Starting from the substrate **1**, C−C bond homolysis and bond rotation simultaneously occur via **TS1**, directly generating intermediate **Int1**.[38] After then, the barrierless radical

recombination of **Int1** via **TS2** produces the *trans* isomer **2**, which is more stable than the *cis* isomer by 2.2 kcal/mol (Figure 8A). In Figure 8A, **TS1**, **Int1**, and **TS2** are open-shell singlet species. These unrestricted DFT calculations give spin-contaminated singlets, with $S^2 = 1.0$, that is they are approximately 50:50 singlet:triplet and the triplet diradical is <0.6kcal/mol or less lower in energy for **TS1**, **Int1** and **TS2**. There is no zwitterionic character in any of these species. For the uncatalyzed *cis* to *trans* isomerization, the rate-limiting step is C−C bond homolysis via **TS1**, and the energy barrier is 40.0 kcal/mol, (Figure 8A), which is in good agreement with the pyrolysis study reported by Doering and Sachdev (Scheme 3). Notably, **TS2** was observed to be lower in energy than **Int1** by 0.3 kcal/mol. Seeking to better understand this outcome, single point calculations in the gas phase without solvation were carried out using the (U)PBE0-D3/def2-TZVPP//(U)B3LYP-D3/def2-SVP level of theory.[42] These calculations indicate that **TS2** is higher in energy than **Int1** by 0.9 kcal/mol in terms of electronic energy, and 0.7 kcal/mol in terms of Gibbs free energy. As such, the solvation correction is believed to be the primary contributor to the energetic ordering presented in Figure 8A. Another minor contributor is the thermal correction to Gibbs free energy, which is responsible for an additional 0.2 kcal/mol difference in free energy between **TS2** and **Int1**.

Next, we studied the Ru-catalyzed isomerization of **1**, and the free energy changes associated with the most favorable pathway are shown in Figure 8B. Starting from **Int2**, complexation-induced homolysis via **TS3** occurs to form radical species **Int3**. In **TS3**, C–C bond cleavage is concerted with a favorable change in oxidation state at the metal center, generating Ru(III) intermediate, **Int3**. From **Int3**, bond rotation occurs via **TS4** to produce **Int4**. After that, C−C bond formation via **TS5** to regenerate closed-shell singlet species **Int5**. **TS3**, **Int3**, **TS4**, **Int4**, and **TS5** are all open-shell singlet species. **Int3**, **TS4**, and **Int4** have the diradical character discussed for the uncatalyzed reaction, whereas **TS3** and **TS5** have S^2 values of 0.7 and the triplets are 3–4 kcal/mol higher in energy. The free energy diagram shown in Figure 8B indicates that the turnover-limiting step is C−C bond cleavage via **TS3**, and the overall barrier for Ru-catalyzed isomerization of **1** is 14.4 kcal/mol (Figure 8B). Overall, these calculations suggest that the Ru catalyst facilitates the C–C σ-bond homolytic cleavage by lowering the activation barrier by 25.6 kcal/mol.

In addition, the thermochemical analysis of the *cis* to *trans* isomerization supports our experimental outcomes. The overall thermodynamic driving force of the isomerization assessed through density functional calculations, ΔG_{calc}, was found to be –2.2 kcal/mol. While examining the reversibility (Scheme 5), the equilibrium constant of the isomerization was measured to be 25; therefore, we measured the difference between the free energies of the *cis* and *trans* stereoisomers, ΔG_{expt}, to be –1.9 kcal/mol.

Concerted versus stepwise mechanisms for metal-catalyzed C-C homolysis.

In surveying the literature on metal-catalyzed C–C bond homolysis in cyclopropanes, we considered whether distinct mechanisms may be operative that vary in the degree of coupling between C–C homolysis step and electron transfer to the substrate carbonyl. As a limiting case of electron transfer preceding C–C cleavage, Yoon has reported that upon coordination of cyclopropyl ketones to La(III) or Gd(III) Lewis acids, outer-sphere electron

transfer generates a ketyl radical intermediate that then induces reversible homolysis of the cyclopropane C–C bond σ-bond.[43,44] C–C bond cleavage that proceeds stepwise through a discrete ketyl intermediate is analogous to the cyclopropylcarbinyl radical anion systems studied by Tanko (Figure 2B). In contrast, the results presented here argue against the formation of a discrete ketyl intermediate prior to C–C bond cleavage. Specifically, the large potential difference between the weakly reducing Ru catalyst ($E_{p/2}$ Ru(III)/Ru(II) = –0.6 V vs Fc^+/Fc)[35] and the ketone substrate in this study ($E_{p/2}$ = –2.6 V vs Fc^+/Fc)[33,34] suggests that electron transfer leading to ketyl formation is highly disfavored on thermodynamic grounds. Rather, in analogy to the X–H bond weakening examples discussed above (Figure 1), we propose that the C–C cleavage event is likely concerted with a favorable change in oxidation state at the metal center, with the latter providing in part the driving force necessary to lower the kinetic barrier to bond scission. If operative, such a mechanism is advantageous in that bond cleavage steps can be facilitated without the requirement for strong electron donors that are sufficiently reducing to formally transfer charge to bound substrates. Other redox catalysis platforms are also known to mediate homolytic cyclopropane activations, often in the context of [3+2] cycloaddition reactions. Recent reports from and Meggers[45] and Procter[46,47] discussed discrete cyclopropylcarbinyl radical anions bound to Rh(III) and Sm(III) catalysts as intermediates competent to promote cyclopropane C–C bond homolysis, while Lin and co-workers[48,49] made use of Ti(IV)/Ti(III) redox catalysis for similar ring-opening radical redox processes, but the concerted versus stepwise nature of the substrate activation step was not specified.

It is possible that these redox catalysts may also operate via concerted mechanisms, with oxidation of metal center being directly coupled to C–C bond cleavage. Delineating this specific aspect of C–C bond homolysis mediated by reducing metals is an interesting question that invites additional study, and has the potential to aid in identifying new opportunities and catalyst platforms for bond-weakening catalysis.

CONCLUSION

In summary, we demonstrate a case study for the complexation-induced bond-weakening of C–C σ-bonds. We obtained mechanistic evidence in support of the following conclusions (Scheme 8). First, the cleavage of the C–C σ-bond is the catalyst turnover limiting step. Second, the C–C bond activation mode is homolytic; we propose benzyl radical species as the intermediates of the observed isomerization reactions. Third, the coordination of the redox-active $Ru(acac)_2$ catalyst to substrate **1** decreases the activation barrier of the C–C bond homolysis by 26 kcal/mol.

To the best of our knowledge, this study is the first ex-ample of quantifying the impact of complexation-induced bond-weakening on the kinetic barrier for catalytic C–C bond homolysis. As shown above, complexation-induced bond-weakening catalysis has the potential to enable the generation of radical intermediates through the homolysis of various types of σ-bonds under mild reaction conditions. Fundamental studies on X-H bond weakening in recent years created has led to subsequent use of these mechanisms in synthesis. We are hopeful that the insights presented here can similarly be employed

as guiding principles for the development of other complexation-induced bond-weakening catalysis and useful C–C bond functionalization technologies.

Supplementary Material

Refer to Web version on PubMed Central for supplementary material.

ACKNOWLEDGMENT

Financial support was provided by Princeton University and the NIH (R35 GM134893). We are also grateful to the National Science Foundation (CHE-1764328 to KNH) for financial support of this research. Calculations were performed on the IDRE Hoffman2 cluster at the University of California, Los Angeles. We thank Willie Wolf, Sangmin Kim, Nick Shin and Elaine Tsui for helpful discussions. We also thank Ken Conover (VT NMR), John Eng (HR-MS), Phil Jeffrey (X-Ray Crystallography), Nick Chiappini (Hammett Study).

REFERENCES

(1). Jun C-H Transition metal-catalyzed carbon–carbon bond activation. Chem. Soc. Rev 2004, 33, 610–618. [PubMed: 15592626]

(2). Souillart L; Cramer N Catalytic C–C Bond Activations via Oxidative Addition to Transition Metals. Chem. Rev 2015, 115, 9410–9464. [PubMed: 26044343]

(3). Chen P.-h.; Billett BA; Tsukamoto T; Dong G "Cut and Sew" Transformations via Transition-Metal-Catalyzed Carbon–Carbon Bond Activation. ACS Catalysis 2017, 7, 1340–1360. [PubMed: 29062586]

(4). Fumagalli G; Stanton S; Bower JF Recent Methodologies That Exploit C–C Single-Bond Cleavage of Strained Ring Systems by Transition Metal Complexes. Chem. Rev 2017, 117, 9404–9432. [PubMed: 28075115]

(5). Wang B; Perea MA; Sarpong R Transition Metal-Mediated C−C Single Bond Cleavage: Making the Cut in Total Synthesis. Angew. Chem. Int. Ed 2020, 59, 18898–18919.

(6). Periana RA; Bergman RG Rapid intramolecular rearrangement of a hydrido(cyclopropyl)rhodium complex to a rhodacyclobutane. Independent synthesis of the metallacycle by addition of hydride to the central carbon atom of a cationic rhodium π-allyl complex. J. Am. Chem. Soc 1984, 106, 7272–7273.

(7). Suggs JW; Jun CH Directed cleavage of carbon-carbon bonds by transition metals: the α-bonds of ketones. J. Am. Chem. Soc 1984, 106, 3054–3056.

(8). Gozin M; Weisman A; Ben-David Y; Milstein D Activation of a carbon–carbon bond in solution by transition-metal insertion. Nature 1993, 364, 699–701.

(9). Chatani N; Ie Y; Kakiuchi F; Murai S Ru3(CO)12-Catalyzed Decarbonylative Cleavage of a C−C Bond of Alkyl Phenyl Ketones. J. Am. Chem. Soc 1999, 121, 8645–8646.

(10). Bart SC; Chirik PJ Selective, Catalytic Carbon−Carbon Bond Activation and Functionalization Promoted by Late Transition Metal Catalysts. J. Am. Chem. Soc 2003, 125, 886–887. [PubMed: 12537484]

(11). Terao Y; Wakui H; Satoh T; Miura M; Nomura M Palladium-Catalyzed Arylative Carbon−Carbon Bond Cleavage of α,α-Disubstituted Arylmethanols. J. Am. Chem. Soc 2001, 123, 10407–10408. [PubMed: 11604000]

(12). Matsumura S; Maeda Y; Nishimura T; Uemura S Palladium-Catalyzed Asymmetric Arylation, Vinylation, and Allenylation of tert-Cyclobutanols via Enantioselective C−C Bond Cleavage. J. Am. Chem. Soc 2003, 125, 8862–8869. [PubMed: 12862483]

(13). Zhao P; Hartwig JF β-Aryl Eliminations from Rh(I) Iminyl Complexes. J. Am. Chem. Soc 2005, 127, 11618–11619. [PubMed: 16104735]

(14). Matsuda T; Shigeno M; Murakami M Asymmetric Synthesis of 3,4-Dihydrocoumarins by Rhodium-Catalyzed Reaction of 3-(2-Hydroxyphenyl)cyclobutanones. J. Am. Chem. Soc 2007, 129, 12086–12087. [PubMed: 17877354]

(15). Nugent WA; RajanBabu TV Transition-metal-centered radicals in organic synthesis. Titanium(III)-induced cyclization of epoxy olefins. J. Am. Chem. Soc 1988, 110, 8561–8562.

(16). Rosales A; Rodríguez-García I; Muñoz-Bascón J; Roldan-Molina E; Padial NM; Morales LP; García-Ocaña M; Oltra JE The Nugent–RajanBabu Reagent: A Formidable Tool in Contemporary Radical and Organometallic Chemistry. Eur. J. Org. Chem 2015, 2015, 4592–4592.

(17). Girard P; Namy JL; Kagan HB Divalent lanthanide derivatives in organic synthesis. 1. Mild preparation of samarium iodide and ytterbium iodide and their use as reducing or coupling agents. J. Am. Chem. Soc 1980, 102, 2693–2698.

(18). Molander GA; Harris CR Sequencing Reactions with Samarium(II) Iodide. Chem. Rev 1996, 96, 307–338. [PubMed: 11848755]

(19). Bezdek MJ; Guo S; Chirik PJ Coordination-induced weakening of ammonia, water, and hydrazine X–H bonds in a molybdenum complex. Science 2016, 354, 730–733. [PubMed: 27846601]

(20). Wang D; Loose F; Chirik PJ; Knowles RR N–H Bond Formation in a Manganese(V) Nitride Yields Ammonia by Light-Driven Proton-Coupled Electron Transfer. J. Am. Chem. Soc 2019, 141, 4795–4799. [PubMed: 30803234]

(21). Chalkley MJ; Oyala PH; Peters JC Cp* Noninnocence Leads to a Remarkably Weak C–H Bond via Metallocene Protonation. J. Am. Chem. Soc 2019, 141, 4721–4729. [PubMed: 30789720]

(22). Semproni SP; Milsmann C; Chirik PJ Four-Coordinate Cobalt Pincer Complexes: Electronic Structure Studies and Ligand Modification by Homolytic and Heterolytic Pathways. J. Am. Chem. Soc 2014, 136, 9211–9224. [PubMed: 24897302]

(23). Bartulovich CO; Flowers RA II Coordination-induced O–H bond weakening in Sm(II)-water complexes. Dalton Trans 2019, 48, 16142–16147. [PubMed: 31549703]

(24). Tarantino KT; Miller DC; Callon TA; Knowles RR Bond-Weakening Catalysis: Conjugate Aminations Enabled by the Soft Homolysis of Strong N–H Bonds. J. Am. Chem. Soc 2015, 137, 6440–6443. [PubMed: 25945955]

(25). Sakai K; Oisaki K; Kanai M Identification of Bond-Weakening Spirosilane Catalyst for Photoredox α-C−H Alkylation of Alcohols. Adv. Synth. Cat 2020, 362, 337–343.

(26). Frey HM The Gas Phase Pyrolyses of Some Small Ring Hydrocarbons. Adv. Phys. Org. Chem 1966, 4, 147–193.

(27). Trautz M; Winkler K Fragen der organischen Chemie. I. Die Geschwindigkeit von Ringsprengungen in Gasen. Trimethylenisomerisation. J. Prakt. Chem 1922, 104, 53–79.

(28). Chambers TS; Kistiakowsky GB Kinetics of the Thermal Isomerization of Cyclopropane. J. Am. Chem. Soc 1934, 56, 399–405.

(29). Rabinovitch BS; Schlag EW; Wiberg KB Geometrical and Structural Unimolecular Isomerization of *Sym*-Cyclopropane-d_2, J. Chem. Phys 1958, 28, 504–505.

(30). Berson JA; Balquist JM The mechanism of pyrolysis of cyclopropanes. Racemization and geometrical isomerization of tetramethylcyclopropane-d6. J. Am. Chem. Soc 1968, 90, 7343–7344.

(31). Carter WL; Bergman RG Optical isomerization during the pyrolysis of alkylcyclopropanes. Evidence for diradical intermediates and an estimate of their relative rates of bond rotation and ring closure. J. Am. Chem. Soc 1968, 90, 7344–7346.

(32). Doering W. v. E. Impact of upwardly revised ΔHf0 of primary, secondary, and tertiary radicals on mechanistic constructs in thermal reorganizations. Proc. Natl. Acad. Sci. U.S.A 1981, 78, 5279–5283. [PubMed: 16593079]

(33). Tanko JM; Drumright RE Radical ion probes. I. Cyclopropyl-carbinyl rearrangements of aryl cyclopropyl ketyl anions. J. Am. Chem. Soc 1990, 112, 5362–5363.

(34). Stevenson JP; Jackson WF; Tanko JM Cyclopropylcarbinyl-Type Ring Openings. Reconciling the Chemistry of Neutral Radicals and Radical Anions. J. Am. Chem. Soc 2002, 124, 4271–4281. [PubMed: 11960456]

(35). Wu A; Masland J; Swartz RD; Kaminsky W; Mayer JM Synthesis and Characterization of Ruthenium Bis(β-diketonato) Pyridine-Imidazole Complexes for Hydrogen Atom Transfer. Inorg. Chem 2007, 46, 11190–11201. [PubMed: 18052056]

(36). Mader EA; Davidson ER; Mayer JM Large Ground-State Entropy Changes for Hydrogen Atom Transfer Reactions of Iron Complexes. J. Am. Chem. Soc 2007, 129, 5153–5166. [PubMed: 17402735]

(37). Roth JP; Mayer JM Hydrogen Transfer Reactivity of a Ferric Bi-imidazoline Complex That Models the Activity of Lipoxygenase Enzymes. Inorg. Chem 1999, 38, 2760–2761. [PubMed: 11671018]

(38). Doering W. v. E.; Sachdev K Continuous diradical as transition state. Internal rotational preference in the thermal enantiomerization and diastereoisomerization of cis- and trans-1-cyano-2-isopropenylcyclopropane. J. Am. Chem. Soc 1974, 96, 1168–1187.

(39). Polar mechanisms are known to be operative in related transformations. Buchert M; Reissig H-U Rearrangement of Donor-Acceptor-Substituted Vinylcyclopropanes to Functionalized Cyclopentene Derivatives: Evidence for Zwitterionic Intermediates. Liebigs Ann 1996, 2007–2013.

(40). Dinçtürk S; Jackson RA; Townson M An improved σ· scale. The thermal decomposition of substituted dibenzylmercury compounds in alkane solutions. J. Chem. Soc., Chem. Comm 1979, 172–174.

(41). Dinçtürk S; Jackson RA; Townson M; Ağirbaş H; Billingham NC; March G Free radical reactions in solution. Part 6. Thermal decomposition of substituted dibenzyl mercurials in solution. An improved σ· scale. J. Chem. Soc., Perkin Trans 2 1981, 1121–1126.

(42). Computational details are included in the Supporting Information

(43). Lu Z; Shen M; Yoon TP [3+2] Cycloadditions of Aryl Cyclopropyl Ketones by Visible Light Photocatalysis. J. Am. Chem. Soc 2011, 133, 1162–1164. [PubMed: 21214249]

(44). Amador AG; Sherbrook EM; Yoon TP Enantioselective Photocatalytic [3 + 2] Cycloadditions of Aryl Cyclopropyl Ketones. J. Am. Chem. Soc 2016, 138, 4722–4725. [PubMed: 27015009]

(45). Huang X; Lin J; Shen T; Harms K; Marchini M; Ceroni P; Meggers E Asymmetric [3+2] Photocycloadditions of Cyclopropanes with Alkenes or Alkynes through Visible-Light Excitation of Catalyst-Bound Substrates. Angew. Chem. Int. Ed 2018, 57, 5454–5458.

(46). Huang H-M; McDouall JJW; Procter DJ SmI2-catalysed cyclization cascades by radical relay. Nat. Catal 2019, 2, 211–218.

(47). Agasti S; Beattie NA; McDouall JJW; Procter DJ SmI2-Catalyzed Intermolecular Coupling of Cyclopropyl Ketones and Alkynes: A Link between Ketone Conformation and Reactivity. J. Am. Chem. Soc 2021, 143, 3655–3661. [PubMed: 33629852]

(48). Hao W; Harenberg JH; Wu X; MacMillan SN; Lin S Diastereo- and Enantioselective Formal [3 + 2] Cycloaddition of Cyclopropyl Ketones and Alkenes via Ti-Catalyzed Radical Redox Relay. J. Am. Chem. Soc 2018, 140, 3514–3517. [PubMed: 29465998]

(49). Hao W; Wu X; Sun JZ; Siu JC; MacMillan SN; Lin S Radical Redox-Relay Catalysis: Formal [3+2] Cycloaddition of N-Acylaziridines and Alkenes J. Am. Chem. Soc 2017, 139, 12141–12144. [PubMed: 28825816]

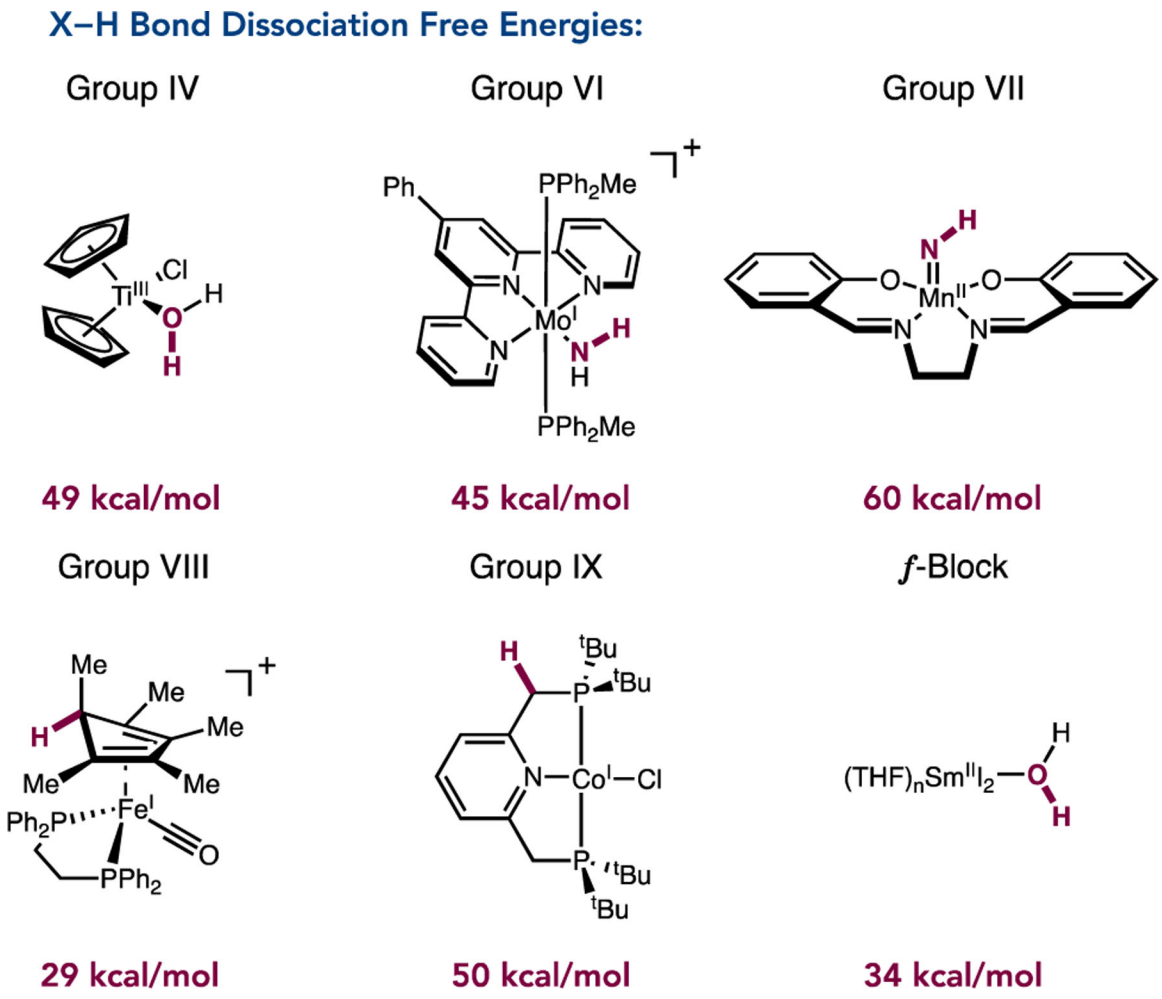

Scheme 1.

C–C Bond Activation Modes Mediated by Transition Metal Catalysts

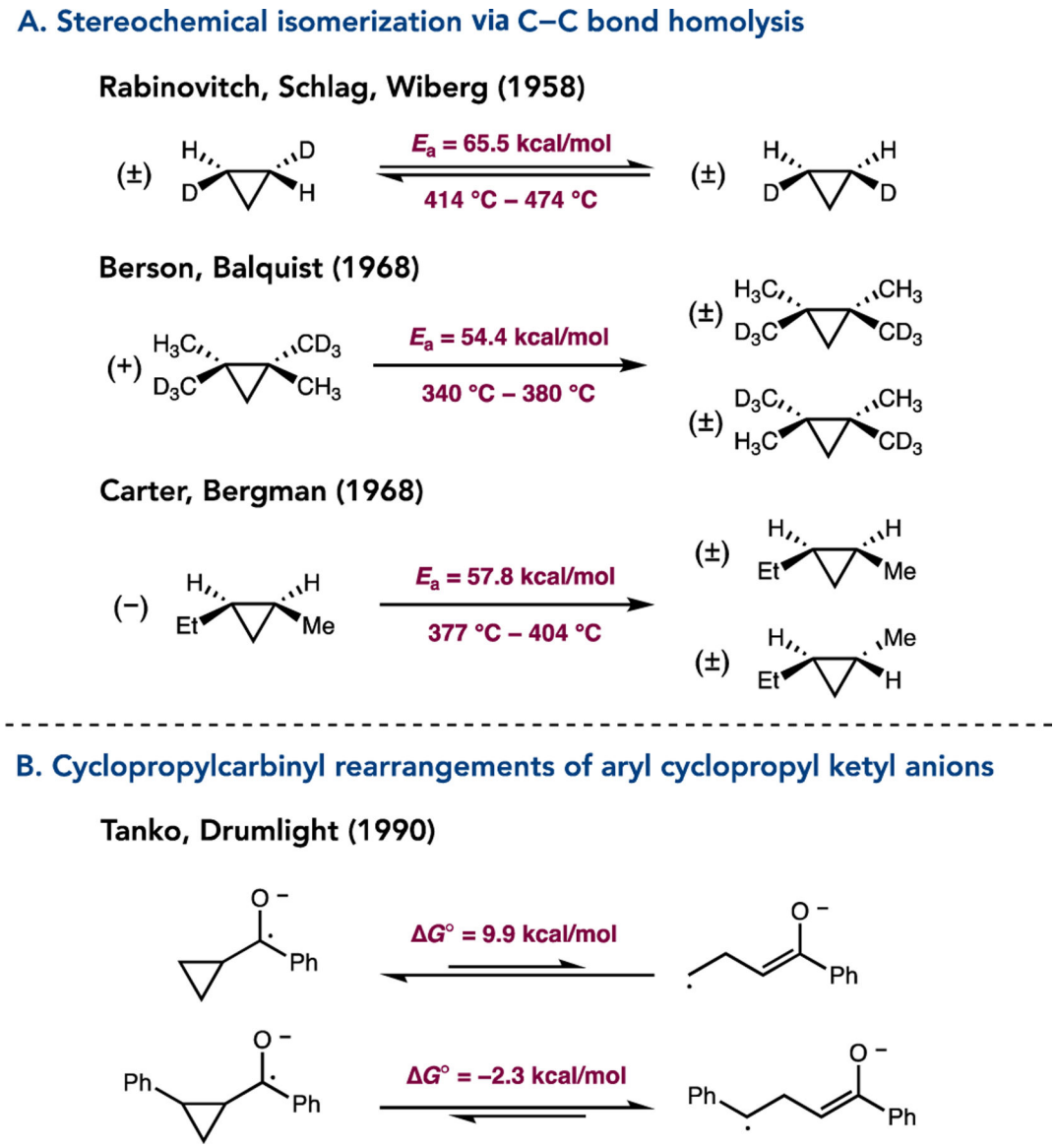

Scheme 2.
Prospective Catalytic Cycle

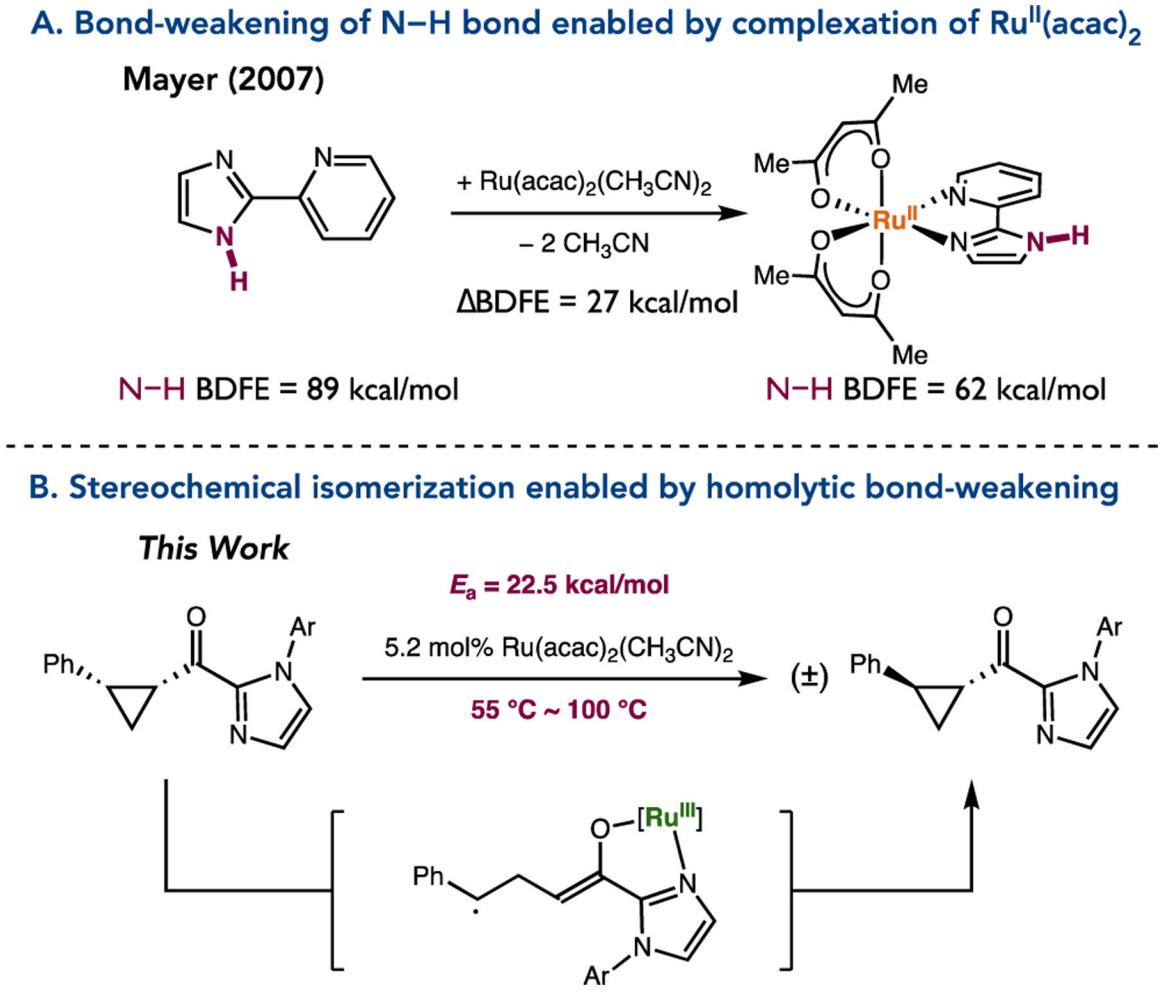

Scheme 3.

Previous Study on the Pyrolysis of an Electronically Analogous Substrate

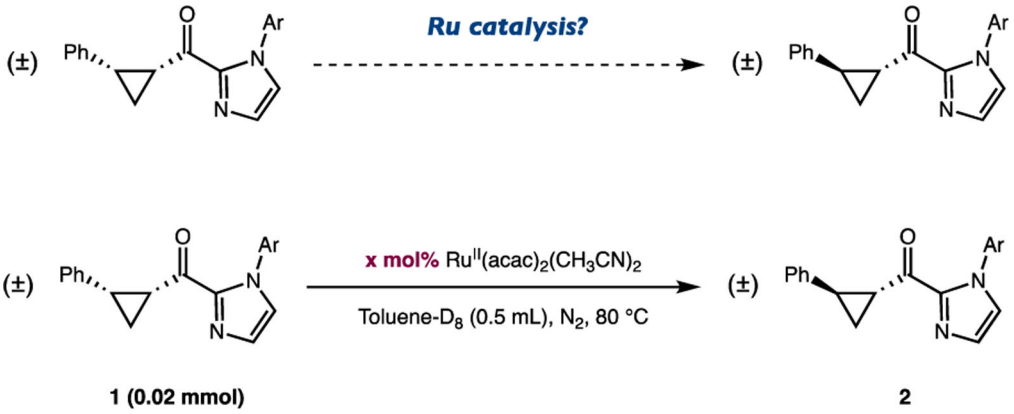

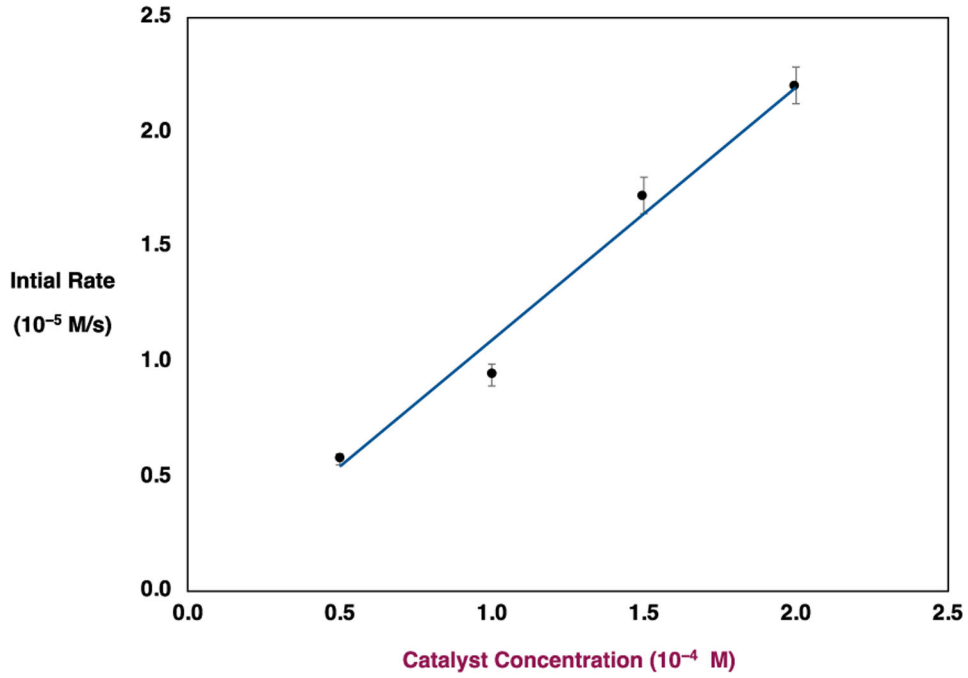

Scheme 4.

Racemization of Enantioenriched *trans* Isomer

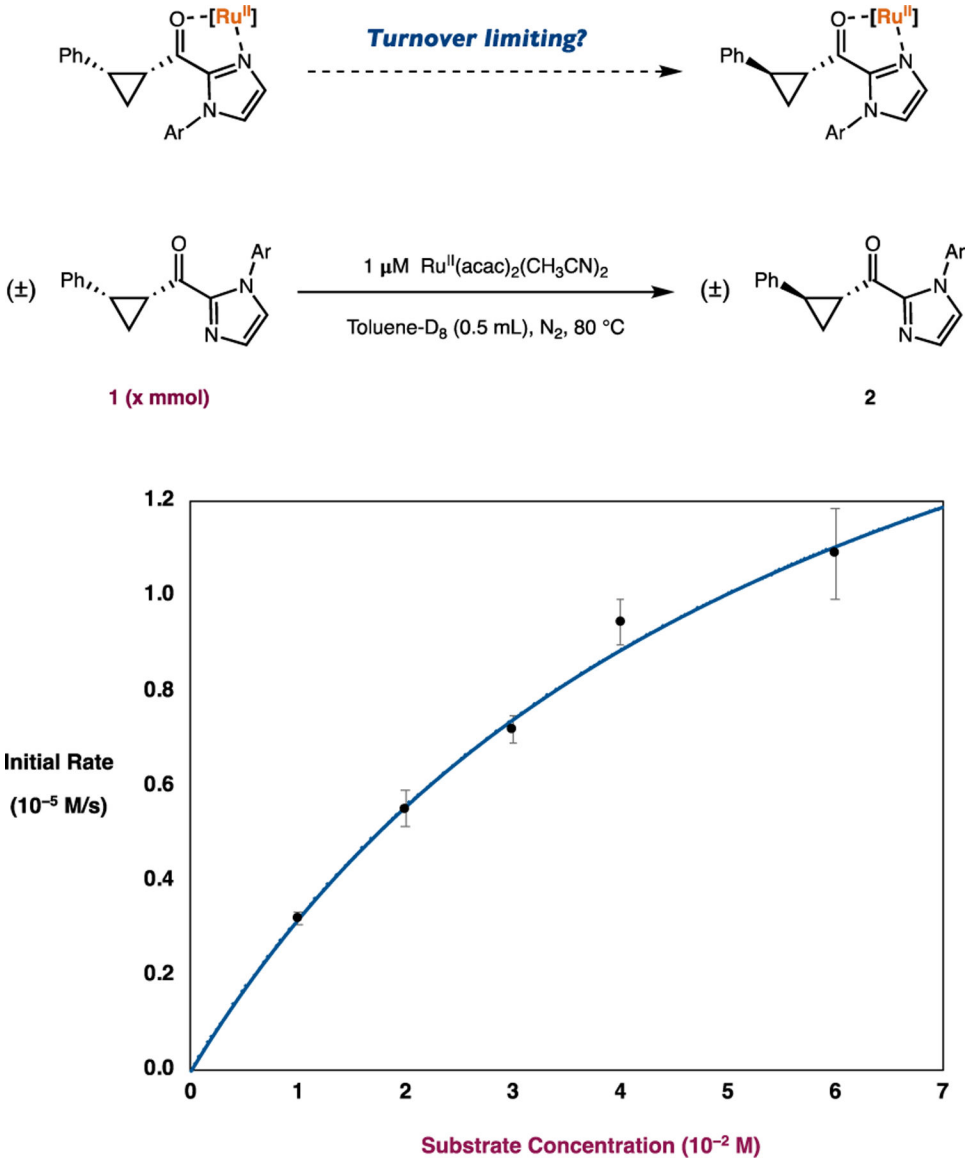

Scheme 5.
Thermodynamically Controlled Isomerization

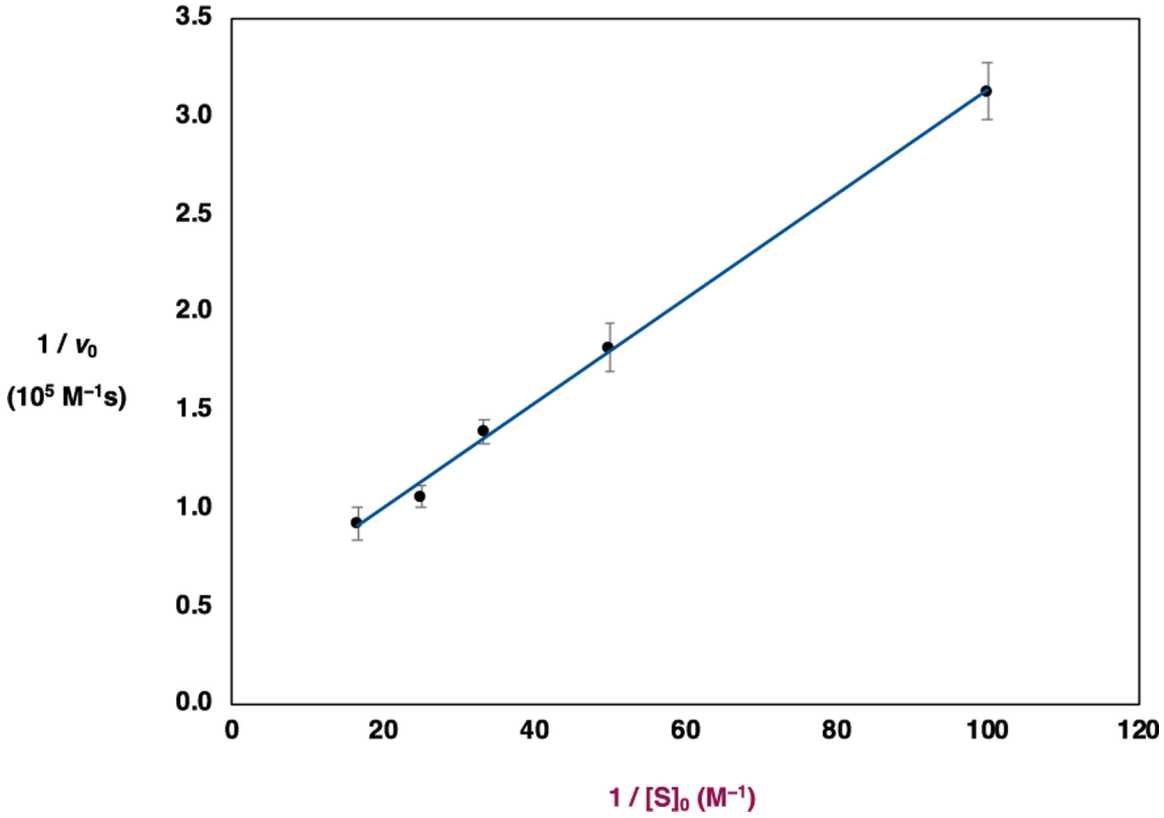

Scheme 6.

Non-stereospecific *cis–trans* Isomerization and Enantiomeric Integrity of Recovered *cis* Isomer

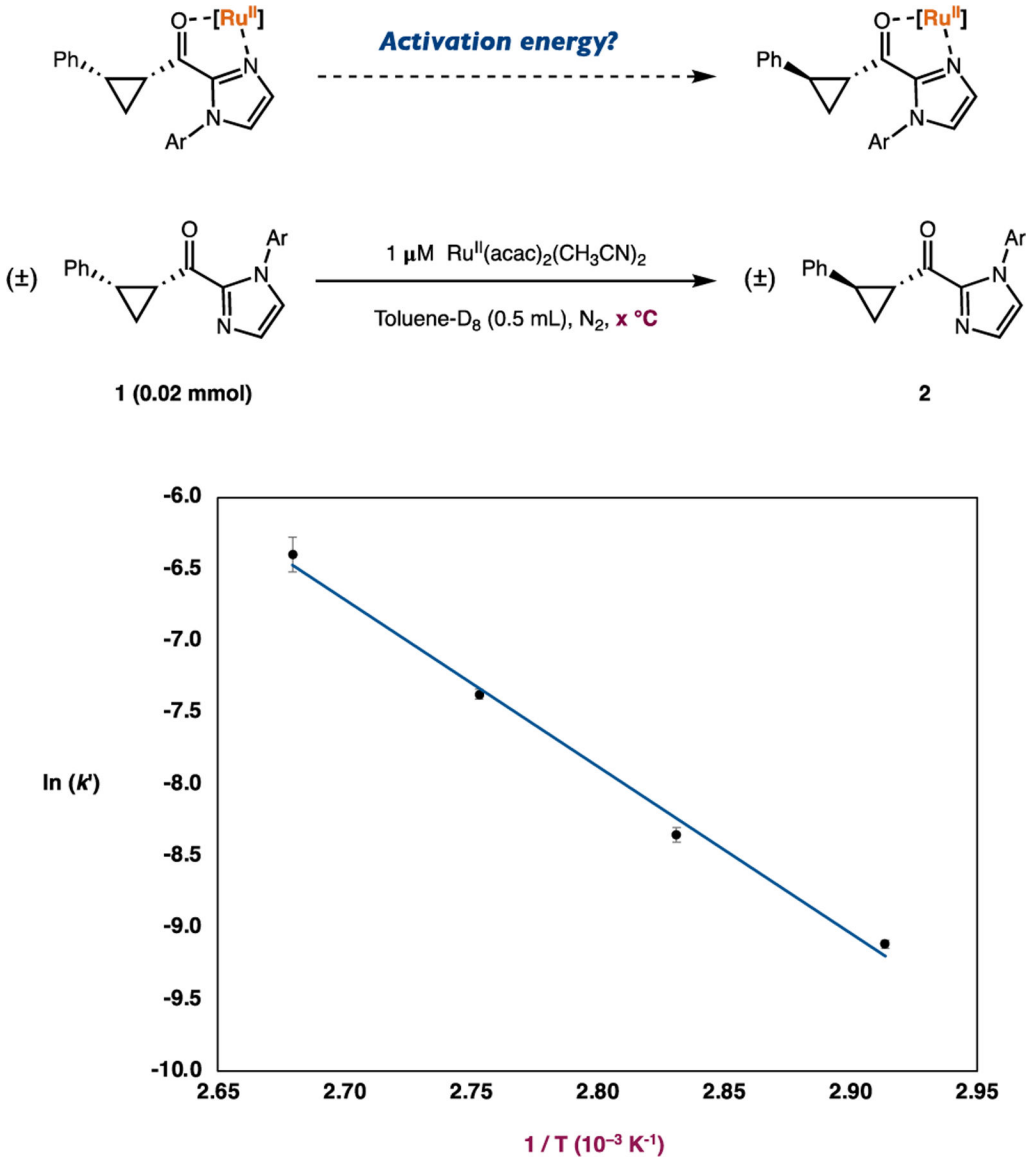

Scheme 7.

Stereospecific *cis–trans* Isomerization of 1,2,3-Trisubstituted Cyclopropane

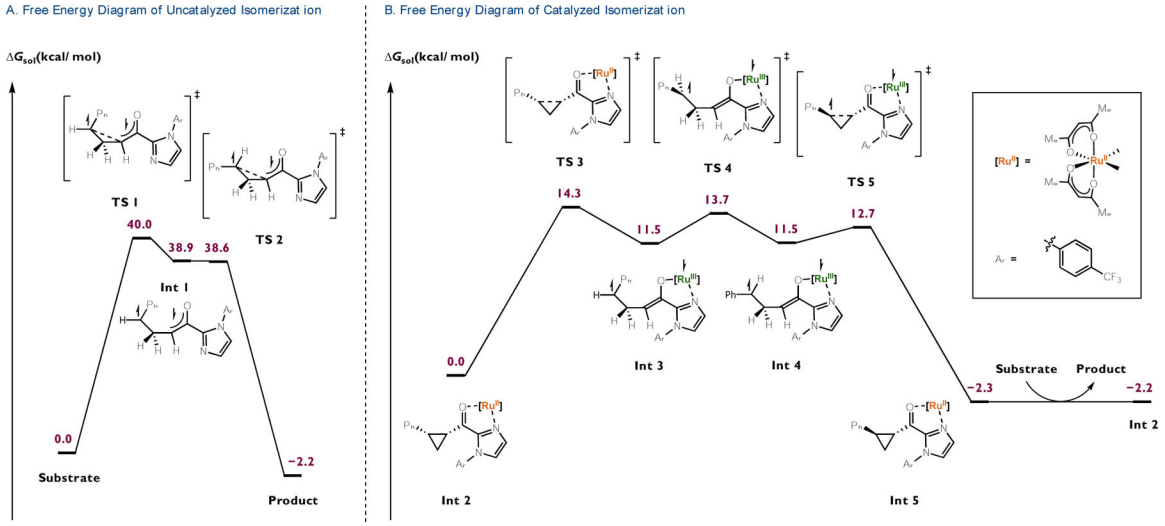

Scheme 8.
Revised Catalytic Cycle

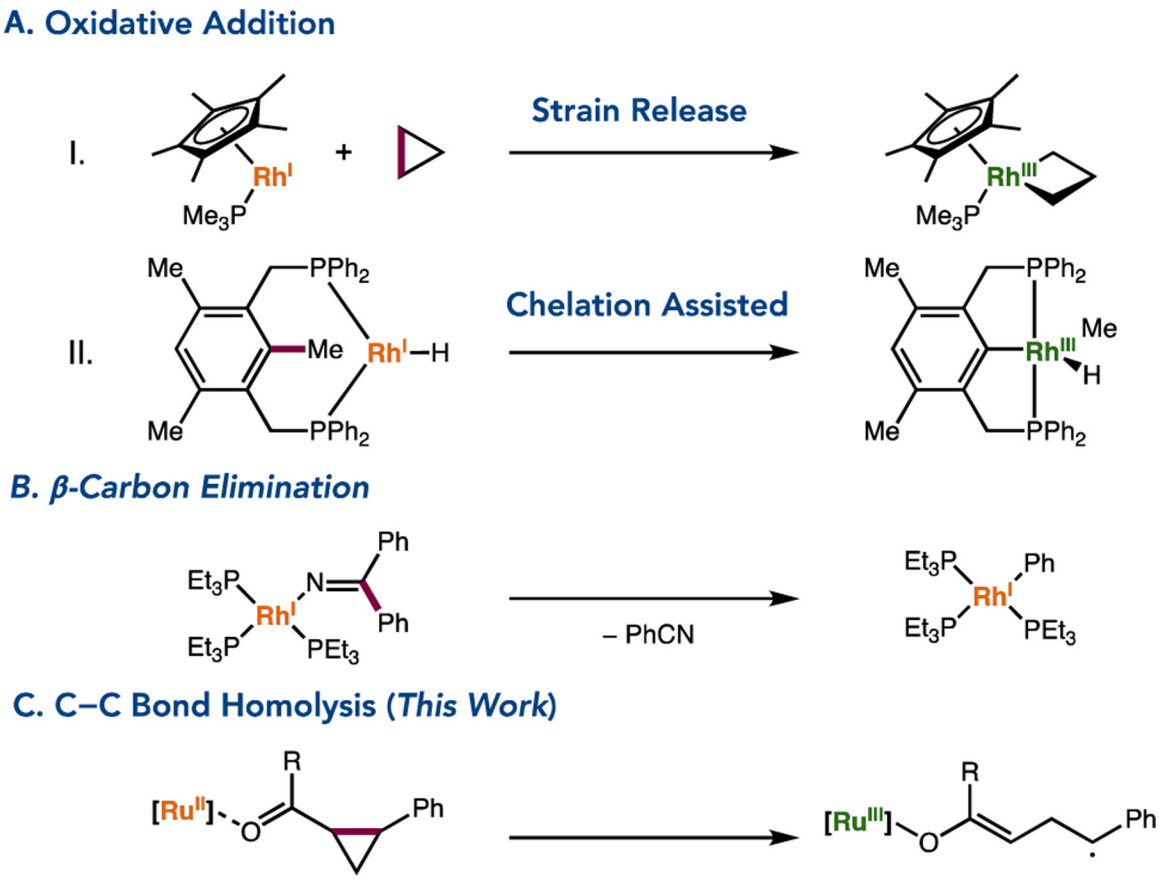

Figure 1.
Examples of complexation-induced X–H bond-weakening.

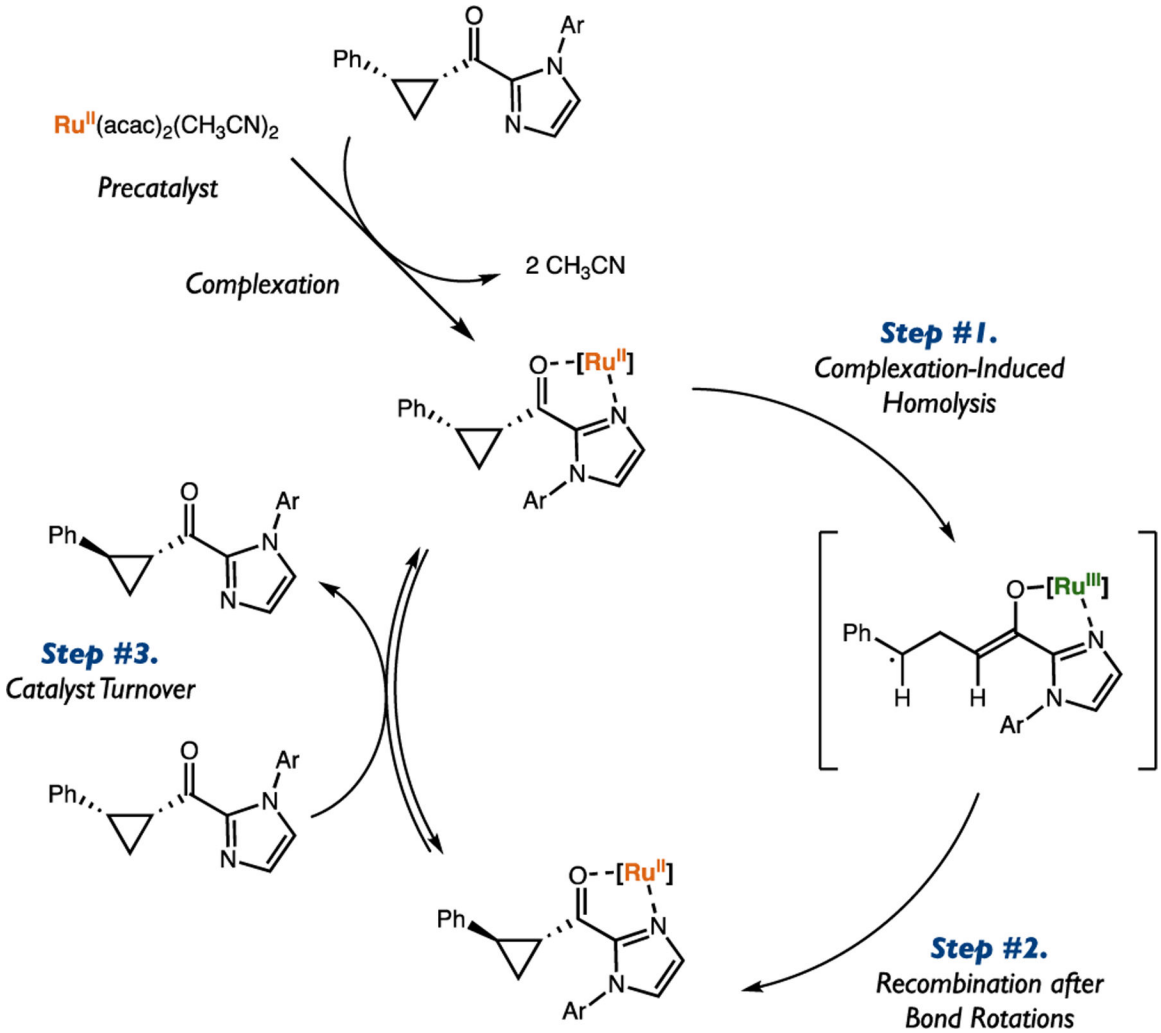

Figure 2.

(A) Early works for reversible ring-opening of cyclopropanes (B) Reversible ring-opening of cyclopropyl ketyl anions.

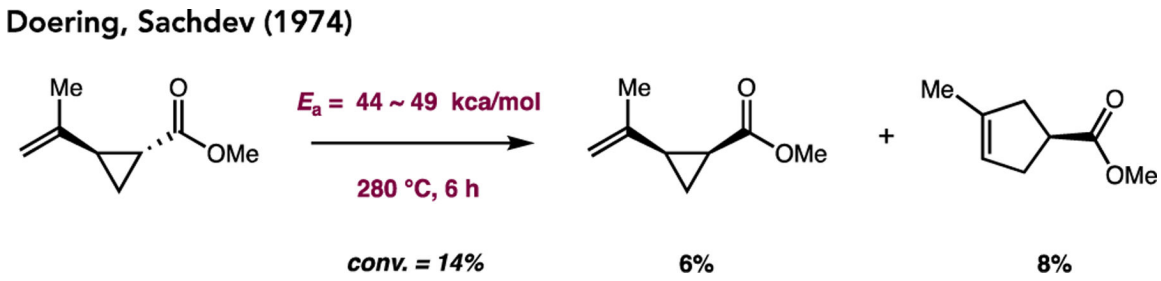

Figure 3.

(A) N–H bond-weakening enabled by Ru(II) complex (B) Catalytic C–C bond homolysis enabled by Ru(II) catalyst.

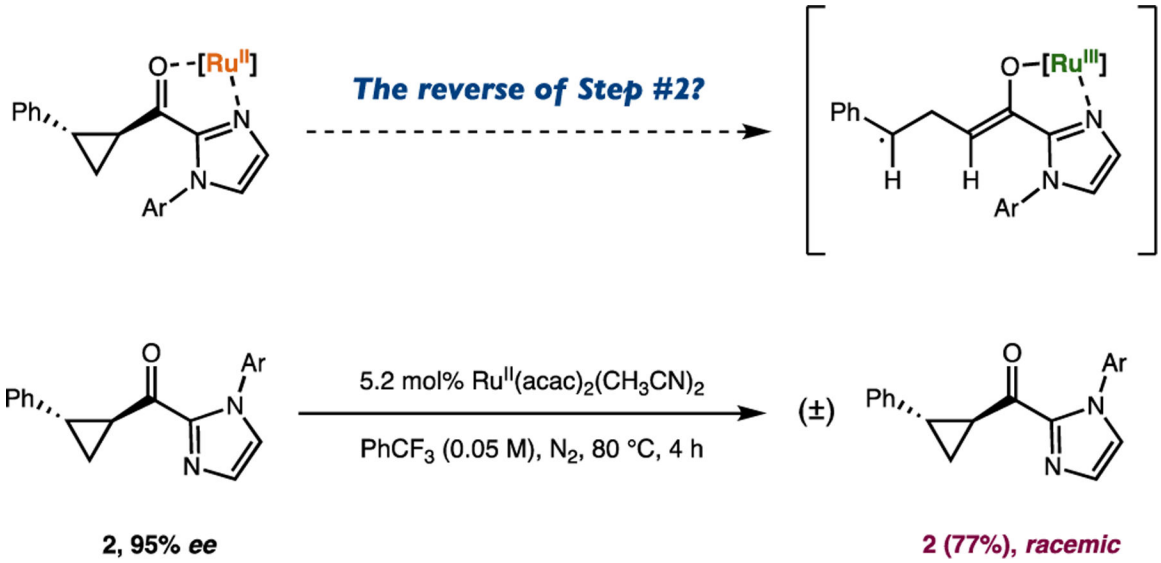

Figure 4.
First-order kinetic dependence on the Ru catalyst concentration.

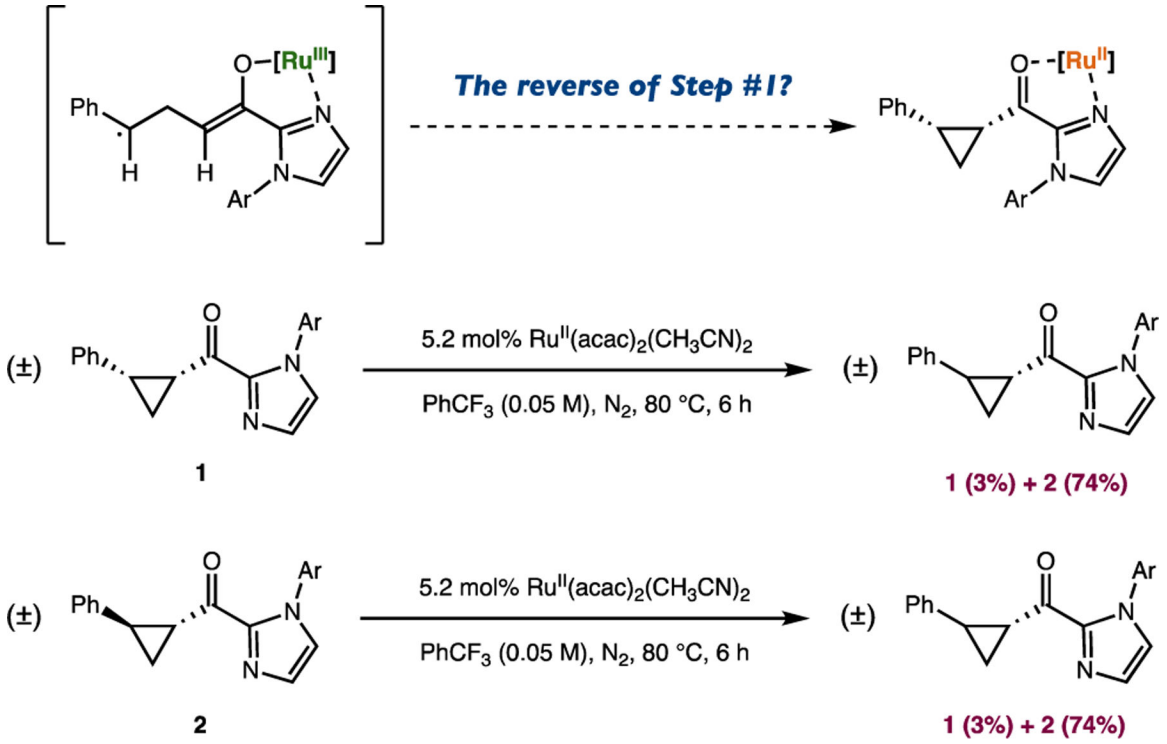

Figure 5.
Saturation kinetics with respect to the substrate concentration.

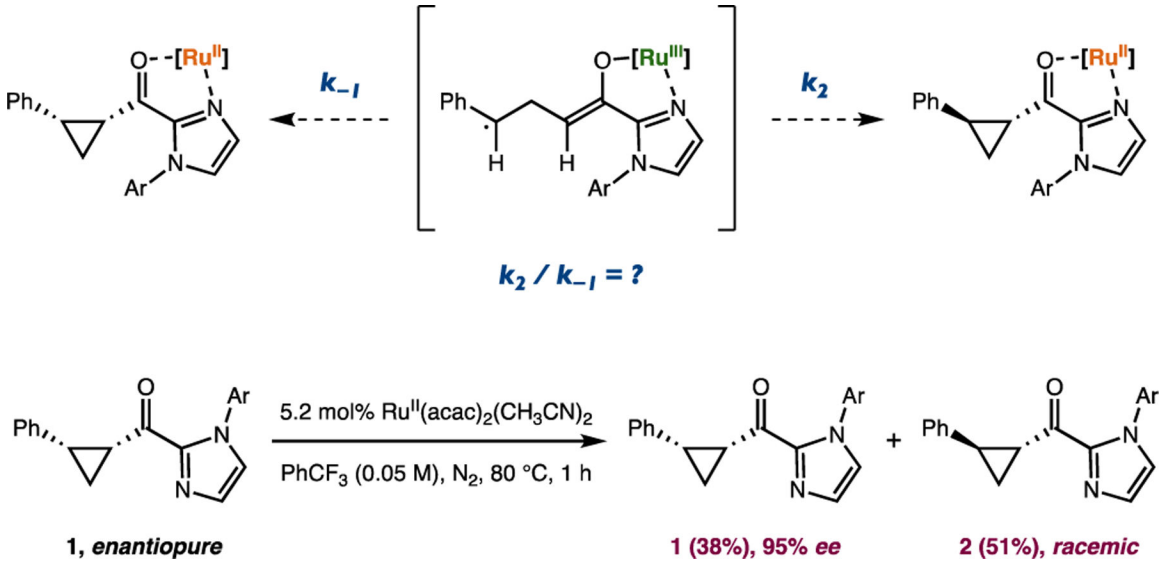

Figure 6.

Arrhenius analysis of $Ru(acac)_2(CH_3CN)_2$-catalyzed *cis* to *trans* isomerization, E_a = 23.2 kcal/mol and ln A = 24.77.

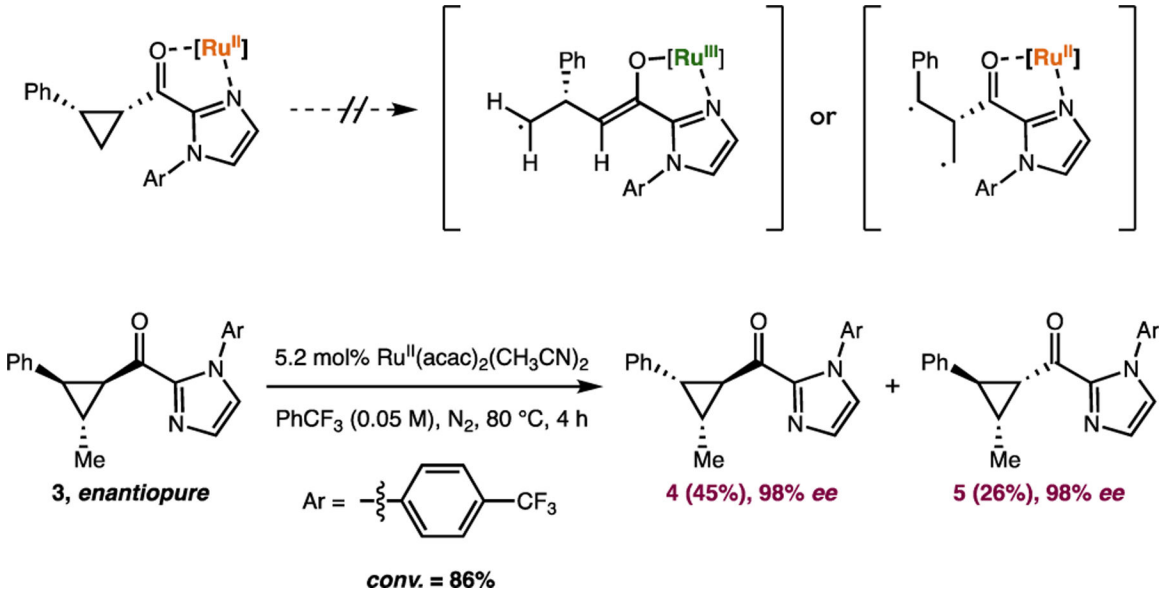

Figure 7.

Lineweaver-Burk analysis of $Ru(acac)_2(CH_3CN)_2$-catalyzed *cis* to *trans* isomerization.

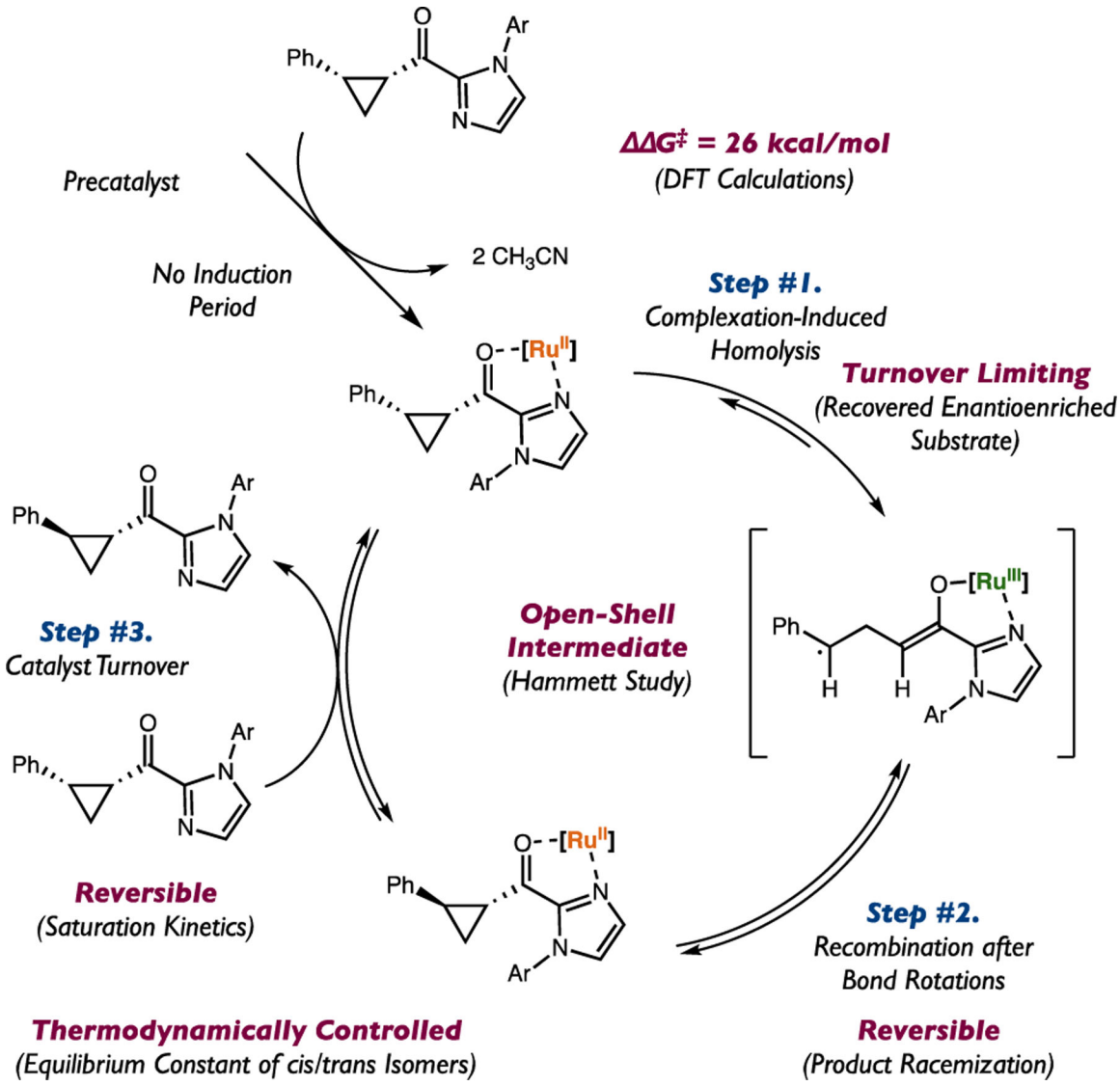

Figure 8.

Free energy diagrams of (A) uncatalyzed and (B) $Ru(acac)_2$-catalyzed *cis* to *trans* isomerization.

Table 1.

Effect of Reaction Parameters[a]

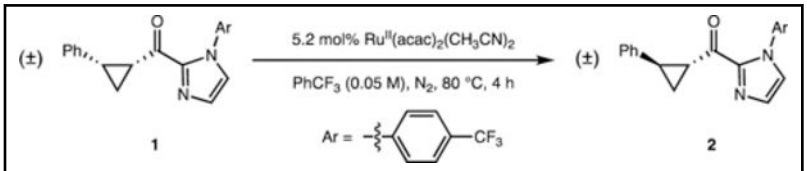

Entry	Variation from above conditions	$[1]/[1]_0$	$[2]/[1]_0$
1	None	9%[b]	81%[b]
2	25 °C	100%	-
3	55 °C	49%	38%
4	100 °C	3%	70%
5	0.025 M	14%	68%
6	0.1 M	4%	75%
7	0 mol%	100%	-
8	2.6 mol%	13%	80%
9	10.4 mol%	3%	73%
10	2 h	13%	69%
11	6 h	3%	73%
12	toluene	5%	79%
13	benzene	6%	68%
14	dichloromethane	28%	20%
15	1,2-dimethoxyethane	4%	81%
16	1,4-dioxane	13%	77%
17	$\{Ru^{III}(acac)_2(CH_3CN)_2\}PF_6$	100%	-

[a] All reactions were performed at 0.05 mmol scale. Yields were determined by ^{1}H NMR analysis of the crude reaction mixture relative to an internal standard.

[b] in triplicate.